DOI 10.1007/s11041-022-00806-w
Metal Science and Heat Treatment, Vol. 64, Nos. 5 – 6, September, 2022 (Russian Original Nos. 5 – 6, May – June, 2022)

UDC 669.1:621.793.795

STRUCTURE OF ALLOY AK10M2N AFTER TENSILE PLASTIC DEFORMATION

K. V. Aksenova,[1] D. V. Zagulyaev,[1] A. A. Klopotov,[2] Yu. F. Ivanov,[3] A. M. Ustinov,[2] and D. S. Yakupov[1]

Translated from *Metallovedenie i Termicheskaya Obrabotka Metallov*, No. 6, pp. 17 – 23, June, 2022.

Original article submitted December 23, 2021.

Silumin AK10M2N is studied in a cast condition and after irradiation with a pulsed electron beam (17 keV, 50 J/cm^2, 3 pulses, 100 sec, 0.3 sec^{-1}). Elemental and phase compositions of the alloy are determined. Structure and the fracture surfaces after uniaxial tension of flat specimens in an INSTRON 3386 machine at a constant rate are studied by scanning electron microscopy and transmission electron diffraction microscopy. It is shown that irradiation of alloy AK10M2N with a pulsed electron beam is accompanied by fusion of a comparatively thin (up to 100 μm) surface layer. Subsequent high-speed crystallization yields a multiphase submicro- and nanocrystalline structure of cellular crystallization. Cast alloy irradiation with an electron beam increases ultimate strength by a factor of 1.8 and elongation by a factor of 2.2. The main causes of this effect are determined.

Keywords: alloy AK10M2N, structure, uniaxial tension, pulsed electron beam, strength, ductility.

INTRODUCTION

Currently aluminum alloys with silicon (silumins) are used extensively in manufacturing various components, starting from everyday engineering components and ending with assemblies used in automobile and aircraft construction that is connected with their low cost, good casting properties, corrosion resistance, and low thermal expansion coefficient [1, 2]. In particular, internal combustion engines pistons and compressors are manufactured predominantly from eutectic and hypereutectic Al – Si-alloys [3, 4]. Unfortunately the surface properties of aluminum alloys sometimes do not correspond to the actual industrial specifications. Without special alloy treatment within a cast structure of aluminum–silicon alloys there is eutectic formation with silicon particles of coarse lamellar shape that considerably reduces component mechanical properties [5]. In resolving this problem scientists operate in the direction of eutectic refinement and a reduction in alloy structure porosity [6, 7].

In the majority of cases in order to improve component service life it is sufficient to strengthen a surface layer. This is connected with the fact that as a rule failure commences actually within a surface and the most intense plastic deformation proceeds within surface layers whose thickness is equal to the grain size. In view of this in order to expand the application field for Al – Si-alloys and to increase the reliability of components manufactured from them a requirement arises for surface modification and an improvement in functional properties. The most promising method for modifying Al – Si-alloys is pulsed electron beam treatment [8, 9]. Surface layer melting by an electron beam followed by crystallization is accompanied by aluminum mixing with silicon and filling pores with melt that facilitates a reduction in the degree of chemical and phase distribution inhomogeneity within material surface layers [10].

A study of Al – 15% Si alloys has shown that treatment with strong current pulsed electron beam increases the ultimate strength in tensile tests by 41.4%, i.e., from σ_r = 140 MPa (initial condition) to σ_r = 195 MPa (after modification) [11]. During irradiation of Al – 10% Si alloy with an electron beam surface nanocrystallization of primary and eutectic Si-phase facilitates an increase in surface layer microhardness and wear resistance by a factor of four [12]. In [13, 14] treatment with a strong current pulsed electron

[1] Siberian State Industrial University, Novokuznetsk, Russia (e-mail: 19krestik91@mail.ru).
[2] Tomsk State University of Architecture and Civil Engineering, Tomsk, Russia.
[3] Institute of High-Current Electronics of the Siberian Branch of the Russian Academy of Sciences (ISÉ SO RAN), Tomsk, Russia.

beam of hypereutectic Al – Si-alloys increased and shifted the Al and Si diffraction peaks. Aluminum lattice spacing decreased due to formation within a liquid layer of supersaturated solid solution based on aluminum. Wear resistance of alloy treated with an electron beam increased by a factor of nine that could be connected with formation of a metastable structures.

Deformation behavior of aluminum alloy has been considered in [15, 16]. It has been demonstrated [15] that alloy 2195-T84 creep strain in tension is significantly higher than in compression. The authors of [16] have established that alloy AlSi10Mg is effectively strengthened by particles that are nanosize Si particles with a maximum value of average phase stress (stress at the Si-phase and Al-matrix interface) of 2 GPa. In this case multistage strain hardening of an aluminum matrix has been observed connected with interaction between dislocations and a cell network boundary.

The aim of the present work is to analyze the elemental and phase composition, defective substructure, and failure surface under uniaxial tension of AK10M2N alloy specimens irradiated by an intense pulsed electron beam.

METHODS OF STUDY

Alloy AK10M2N was studied in a cast condition with the following chemical composition, wt.%: (9.5 – 10.5) Si, (2.0 – 2.5) Cu, (0.8 – 1.2) Ni, (0,9 – 1.2) Mg, up to 0.6 Fe, up to 0.05 Mn, up to 0.05 Ti, up to 0.05 Pb, up to 0.06 Zn, up to 0.01 Sn, balance Al (GOST 30620–98). Test specimens in the form of two-sided blades were prepared by electro-erosion cutting of a massive ingot in accordance with GOST 1497–84. The workpiece specimens obtained were subjected to polishing with diamond paste with a different fineness. Before testing specimens had the following dimensions: thickness 2.3 mm, width 9.1 mm, and gage length 16.0 mm.

Polished specimens were separated into two batches. The first batch remained in the original (cast) condition. The working region of a second batch blade was irradiated from two sides with a pulsed electron beam in a SOLO (ISÉ SO RAN) unit [17]. It includes: a pulsed electron source based on a plasma cathode with cellular stabilization of plasma boundaries; a supply unit; an electron source supply unit; a vacuum chamber with an inspection window and two-coordinate table manipulator on which a plasma source of electrons and an irradiated specimen were placed; a control and diagnosis system for electron source and beam parameters. The main electron beam parameters, determining the temperature profile of the surface layer heated zone and correspondingly the nature and structure of phase transformation kinetics, are energy density within an electron beam, duration, amount and sequence frequency of radiation pulses. The following electron beam parameters were used in the work: accelerated electron energy 17 keV, electron beam energy density 50 J/cm^2; pulse duration 100 μsec; number of pulses 3; pulse sequence frequency 0.3 sec^{-1}; residual gas (argon) pressure in the unit working chamber 2×10^{-2} Pa. Silumin mechanical tests were accomplished by uniaxial tension of flat proportional specimens in an INSTRON 3386 machine with a constant rate of 1.25 mm/min, and after each irradiation regime no fewer than three specimens were tested.

A study of elemental and phase compositions of a defective sub-stricture (structure having disruption in the crystal lattice structure) and failure surface was performed by scanning electron microscopy (Philips SEM-515 with EDAX ECON IV microanalyzer), and transmission electron diffraction microscopy using a JEOL JEM 2100F microscope, making it possible to accomplish highly selective scanning by an electron beam (STEM analysis), to conduct analysis of electron energy loss (EELS), and to study the elemental composition of foil by an x-ray radiation energy analysis dispersion method. A study of the state of alloy crystal lattice was accomplished by x-ray phase analysis (Shimadzu XRD 6000 x-ray diffractometer, copper K_α-radiation). Analysis of the phase composition was conducted using PDF 4+ database, and also a POWDER CELL 2.4 full-profile analysis program.

RESULTS AND DISCUSSION

In our previous work [18, 19] it has been stated that alloy AK10M2H in the original (cast) condition is polycrystalline consisting of grains of solid solution based on aluminium ($Al_{so.s}$) and lamellar Al – Si-eutectic. The size of $Al_{so.s}$ grains within limits from 75 to 20 μm, and eutectic grains vary from 55 to 80 μm. As for many other alloys of the Al – Si system [20] alloy AK10M2H has presence of intermetallic inclusions being of equiaxed shape ("Chinese hieroglyphs", needles,, globules, plates). Presence of silicon plates within the alloy and intermetallic phase inclusions leads to an increase in brittleness.

Mechanical tensile tests for silumin specimens showed that the most increase in ductility and strength indices is provided by an electron beam radiation regime with parameters 17 keV, 50 J/cm^2, 100 μsec, 3 pulses, 0.3 sec^{-1}. As a result of this alloy ultimate strength increases by a factor of 1.8 and relative elongation by a factor of 2.2 compared with similar properties of cast alloy.

Results are provided in Fig. 1 of a failure surface and in Fig. 2 of the structure of a surface layer after alloy AK10M2N irradiation by a pulsed electron beam.

In studying a specimen failure surface it has been established that testing alloy in a cast conditions forms a brittle fracture (Fig. 1*a*). It is evident that this is connected within the material of coarse silicon inclusions and intermetallics.

Research has shown that irradiation of a specimen with a pulsed electron beam is accompanied by high-speed melting of a surface layer up to 90 μm thick. As a result of subsequent high-speed crystallization due to heat removal into an integral cold volume there is formation of acellular type structure (Fig. 2*a*).

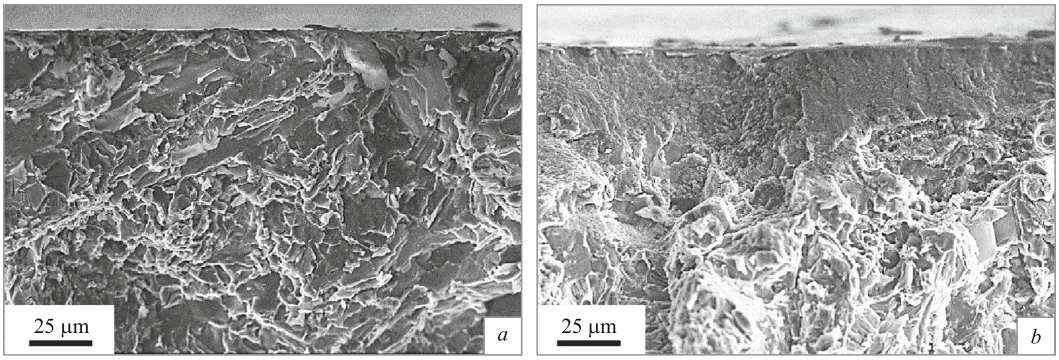

Fig. 1. Alloy AK10M2N structure (electron microscope) failure surface in cast condition (*a*) and after irradiation by a pulsed electron beam (*b*).

By methods of microdiffraction analysis (mapping) with a subsequent indicator microelectron pictures and use of dark field analysis methods [21] a study was made of a silumin surface layer phase composition modified by a pulsed electron beam. It has been established that the crystallization cells with sizes of 0.5 – 0.8 μm form a solid solution based

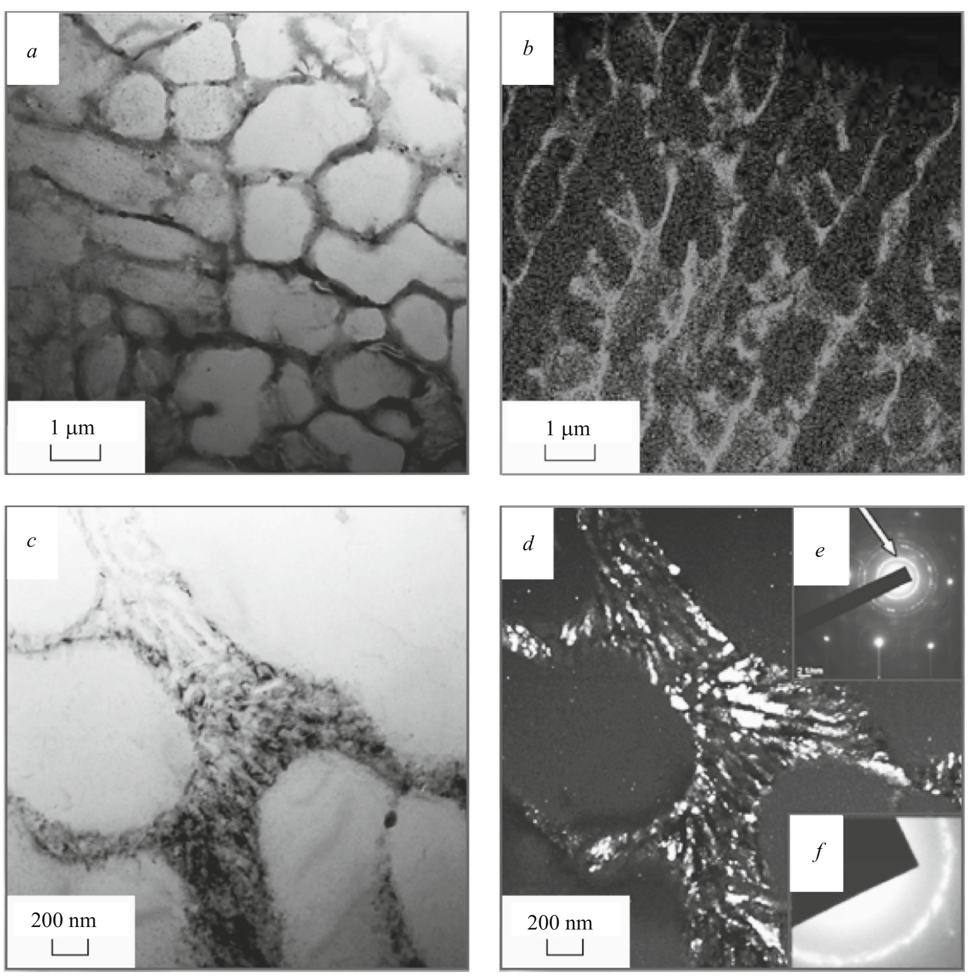

Fig. 2. Structure of the surface layer of the AK10M2N alloy after irradiation by a pulsed electron beam: *a*, *c*) in a bright field; *b*) in the characteristic x-ray radiation of silicon atoms; *d*) in a dark field in a reflection in [111]Si; *e*) microelectron diffraction pattern (the arrow indicates the reflection in which the dark field was obtained in Fig. 2*d*); *f*) fragment of the microelectron diffraction pattern in Fig. 2*e*.

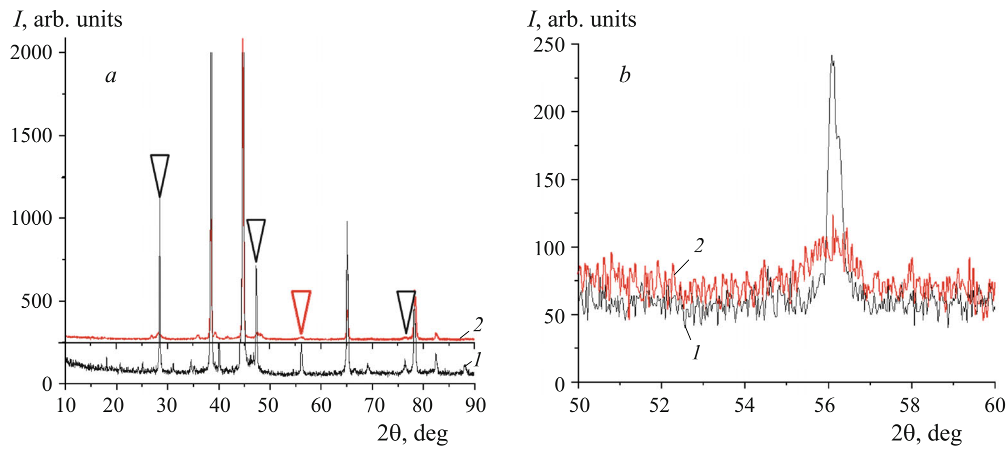

Fig. 3. Fragments of x-ray diffraction patterns obtained from alloy AK10M2N flat proportional specimens failed as a result of uniaxial tension after casting (*1*) and irradiation by a pulsed electron beam (*2*): *a*) general view (points show silicon diffraction maxima); *b*) x-ray diffraction pattern section with silicon diffraction line (311).

on aluminum. Along cell boundaries there is formation of extended second phase layers enriched predominantly with silicon atoms (Fig. 2*b*). Layers separating cells have a nanocrystalline structure. Dimensions of crystals vary within wide limits, i.e., from 4 to 15 nm (Fig. 2*c* and *d*).

Microelectron diffraction patterns, obtained from specimens with this structure have a circular shape (Fig. 2*e*). Diffraction rings are superposition of point reflections and a diffuse halo (Fig. 2*f*). Evidently the latter is caused by presence of silicon, being in an amorphous condition, and interlayers separating cells. It should be noted silicon inclusions and intermetallics of acicular shape, typical for the cast condition structure, are not observed in this case.

Therefore, electron beam treatment of alloy AK10M2N is accompanied by a change in materials irradiated layer phase composition and in fact absence of intermetallic phase.

It has been established by x-ray phase analysis that deformation of alloy specimens during testing in uniaxial tension to failure does not lead to a qualitative change in the material phase composition, i.e., the main phases are solid solution based on aluminum and silicon (Fig. 3*a*). Cast alloy deformation is accompanied by an insignificant reduction in silicon content that may be due to dispersion of its crystals. Simultaneously with this an increase in recorded in the aluminum crystal lattice spacing from 0.40460 nm in the cast condition to 0.40502 nm after deformation. This may be connected with deformation alloying of an aluminum crystal lattice with silicon atoms and other alloying elements that form intermetallics.

As results of x-ray structural analysis have shown deformation of silumin specimens previously irradiated by a pulsed electron beam is accompanied by an increase in silicon content within alloy from 6.9 wt.% in an irradiated condition to 10.7 wt.% after deformation. Simultaneously with this deformation of irradiated alloy leads to a reduction in aluminum crystal lattice spacing from 0.40475 nm in an irradiated condition to 0.40435 nm after failure. An increase in relative silicon content during material deformation is accompanied by blurring diffraction lines for this phase (Fig. 3*b*). This may be caused by formation of nanosize silicon particles as a result of deformation induced transition of an amorphous condition into crystalline. This assumption agrees with results of x-ray phase analysis pointing to an increase in relative silicon content in alloy after specimen failure.

Therefore, results obtained by x-ray phase analysis make it possible to provide a basis for concluding that alloy AK10M2N deformation in cast and irradiated conditions develops by different mechanisms. Deformation of cast specimens is accompanied by an insignificant reduction in the relative silicon content within material, and an increase in solid solution based on aluminum crystal lattice spacing. Deformation of alloy irradiated with a pulsed electron beam is accompanied by an increase in the relative silicon content and a reduction in aluminum crystal lattice spacing.

A defective silumin structure, formed during plastic tensile deformation for specimens irradiated by a pulsed electron beam have been studied by transmission electron diffraction microscopy methods (Fig. 4). It has been established that tensile plastic deformation does not lead to failure of the cellular high-speed crystallization structure (Fig. 4*a* and *b*). Within the volume of cells a dislocation sub-structure is observed in the form of randomly distributed dislocations (Fig. 4*b*). Scalar density of dislocations is high and reaches of $(1-2) \times 10^{10}$ cm^{-2}.

Deformation of alloy AK10M2N specimens is accompanied by breakdown of solid solution based on aluminum and separation within the volume of crystal cells predominantly along second phase particle dislocation lines of spherical shape with sizes of 508 nm (Fig. 4*c* and *d*). The phase composition of particles was studied by analyzing microelectron patterns and dark field images (Fig. 5). As a result of

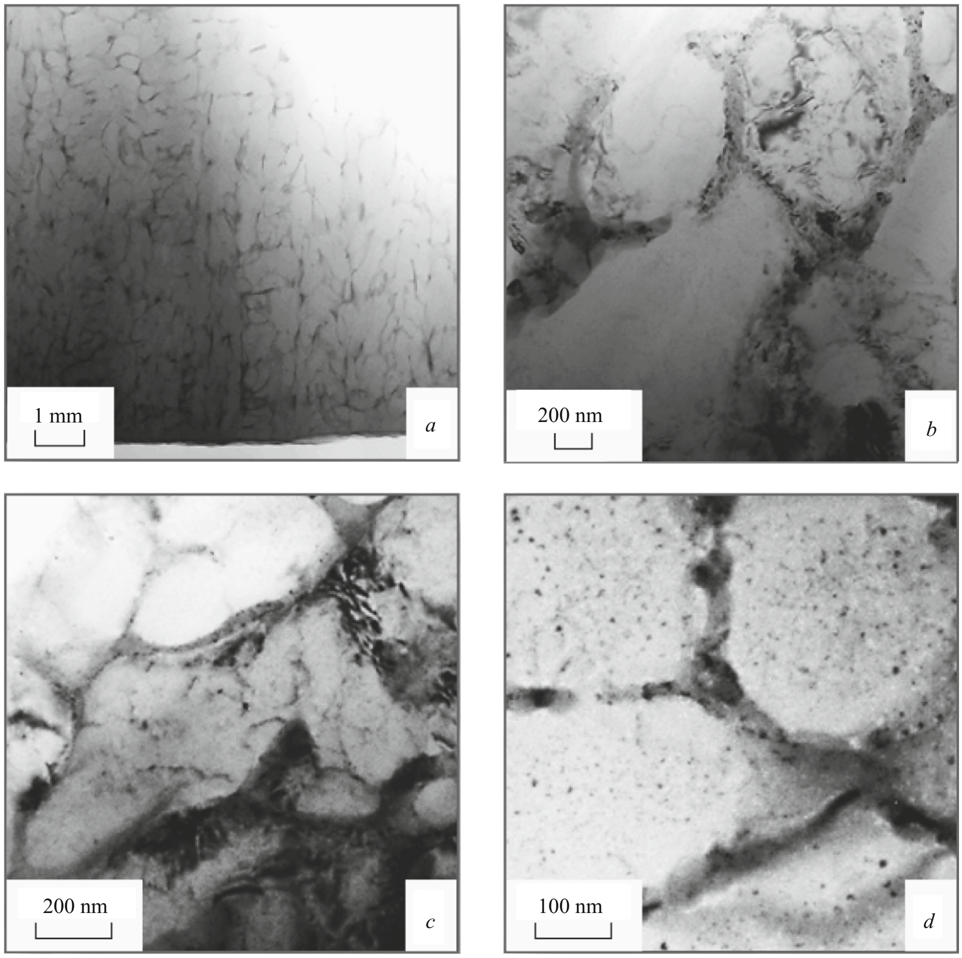

Fig. 4. Structure of the AK10M2N alloy after irradiation by a pulsed electron beam and subsequent tensile deformation to failure: *a*, *b*) cellular structure; *c*, *d*) particles of the second phase in cells on dislocations; *a*, *c*) STEM analysis; *b*, *d*) TEM analysis.

microelectron pattern indications it has been established that the main phase located along crystallization cell boundaries is silicon (see Fig. 5*c*). Within the volume of crystallization cells particles of complex composition $Al_{23}CuFe_4$ (Fig. 5*d*) are observed.

Therefore, tension for specimens of alloy AK10M2N irradiated by a pulsed electron beam is accompanied by material strain ageing with separation of nanosize second phase particles. It may be proposed that one of the mechanisms for increasing the strength of irradiated alloy (with respect to cast condition) is precipitation hardening caused by separation of nanosize second phase inclusions being a hindrance for dislocation movement.

The specific role of high-speed crystallization cells in increasing silumin mechanical properties, irradiated by a pulsed electron beam, is clearly revealed in studying an alloy failure surface. Analysis of fractograms presented in Fig. 1*b* points to formation within specimens of a multilayer structure differing with respect to failure mechanism. Within a surface layer up to 100 μm thick a fracture has a microcrystalline structure with a facet size of 300 – 500 nm. Therefore, the fracture structure coincides with that formed within alloy as a result of material preliminary treatment by a pulsed electron beam. Consequently, failure of a layer irradiated by a pulsed electron beam is accomplished by movement of microcracks along a crystallization cell interface, i.e., there is formation of an intercrystalline (intergranular) fracture. With intercrystalline fracture failure is accomplished by crack propagation predominantly over grains boundaries as a result of their lower strength compared with the body of grains. Intercrystalline failure is facilitated by segregation of impurities over grain boundaries, formation of brittle intergranular interlayers of intermediate phases, absorption reduction of strength, a reduction (with cold brittleness) or an increase (with hot shortness) in hot shortness temperature. It is apparent that in the material tested by us the main reason for formation of intercrystalline fracture is in fact enrichment of grain boundaries with impurity elements and alloying element atoms, and also formation of second phase inclusions that is undoubtedly demonstrated by results of analyzing

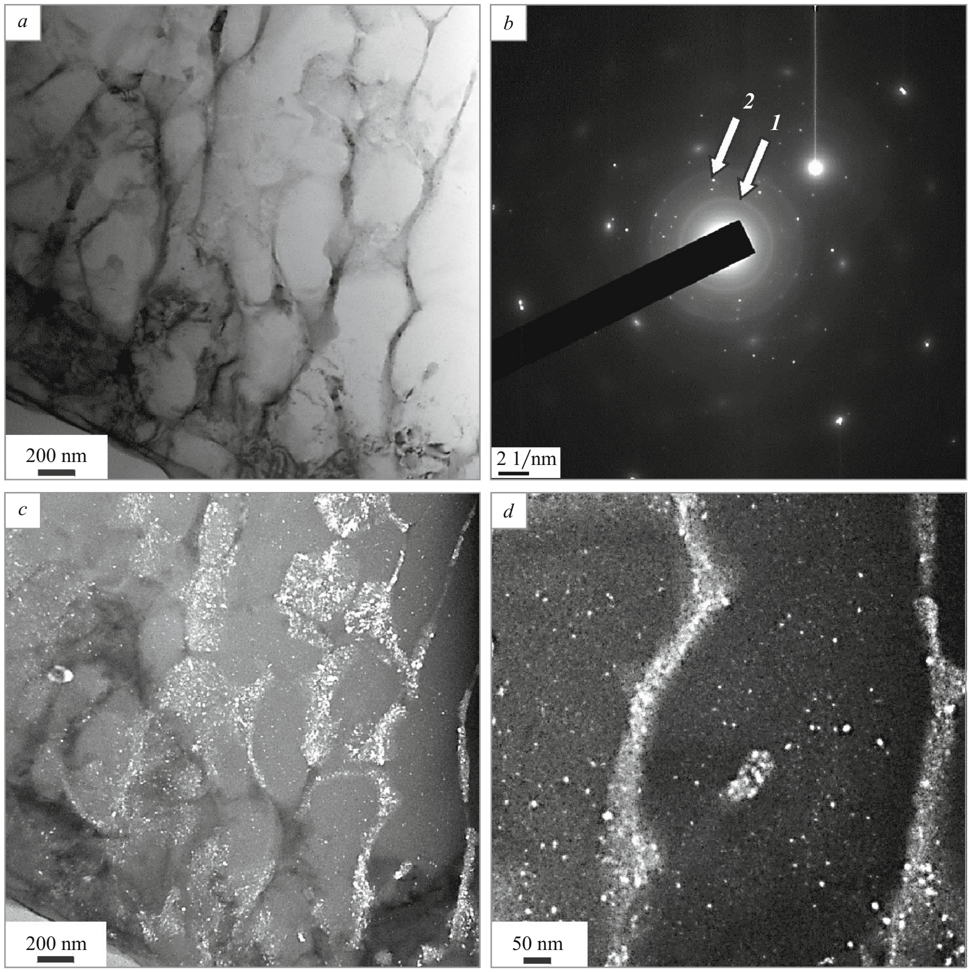

Fig. 5. Electron microscope image of alloy AK10M2N structure irradiated by a pulsed electron beam and failed as a result of deformation in tension: *a*) light field; *b*) micro-electron picture (*1*, *2* are reflections in which the dark field is obtained in Fig. 5*c* and 5*d* respectively); *c*, *d*) dark field in reflections [111] Si and [222] $Al_{23}CuFe_4$ respectively.

specimen structure obtained by transmission electron microscopy methods (Fig. 3). At a considerable distance from a specimen surface a structure is revealed formed during material brittle failure similar to that formed during alloy failure in a cast condition (Fig. 1).

Therefore, the following reason may be distinguished for an increase in alloy AK10M2N ductility properties irradiated by a pulse electron beam: *1*) dispersion of a surface layer structure by dissolution and subsequent high-speed crystallization of silicon crystallites and intermetallic inclusions; *2*) formation within a surface layer with thickness up to 100 μm of submicron and nanocrystalline structure of high-speed aluminum cellular crystallization; *3*) stabilization of second phase precipitate nanosize cell boundaries. An increase in irradiated alloy strength (with respect to a cast condition) due to precipitation hardening is caused by separation of nanosize second phase inclusions being a hindrance for dislocation movement.

CONCLUSIONS

A study has been made in the work of the effect of treatment by an intense pulsed electron beam on structure, change in elemental and phase composition of alloy AK10M2N subjected deformation by uniaxial tension.

Irradiation of alloy AK10M2N by a pulsed electron beam (17 keV, 50 J/cm^2, 100 μsec, 3 pul., 0.3 sec^{-1}) is accompanied by melting of a comparatively thin (up to 100 μm) surface layer. Subsequent high speed crystallization leads to formation of submicron and nanocrystalline multiphase structure of cellular crystallization. Crystallization cell structure, whose size varies within the limits of 0.5 – 0.8 μm, is a solid solution based on aluminum. An interlayer separating cells, has a nanocrystalline structure with crystallite sizes from 4 to 15 nm.

Irradiation of a silumin specimen surface by a pulsed electron beam facilitates an increase in material ultimate strength by a factor of 1.8, relative elongation by a factor of 2.2, compared with similar properties for alloy in a cast condition.

Failure of alloy AK10M2N specimens in a cast condition is accompanied by brittle fracture formation that is apparently connected with presence within it of coarse silicon and intermetallic inclusions. Failure of alloy irradiated by a pulsed electron beam is accomplished by microcrack propagation along cell crystallization interfaces, i.e., intercrystalline (intergranular) fracture is formed.

Deformation of alloy AK10M2N in cast and irradiated conditions develops by different mechanisms. Deformation of cast specimens is accompanied by an insignificant reduction in relative silicon content within solid solution within an aluminum base, and an increase in crystal lattice spacing. Deformation of alloy previously irradiated by a pulsed electron beam is accompanied by an increase in relative silicon content and a reduction in aluminum crystal lattice spacing.

The main reasons have been revealed for an increase in ductility properties of alloy AK10M2N irradiated by a pulsed electron beam: *1*) dispersion of the surface layer structure by dissolution and subsequent high-speed crystallization of silicon crystallites and intermetallic inclusions; *2*) formation within a surface layer up to 100 μm thick of a submicro- and nanocrystalline structure with high-speed crystallization of aluminum; *3*) grain boundary stabilization by nanosize second phase precipitates. An increase in irradiated alloy strength (with respect to cast condition) is due to precipitation hardening caused by secondary phase inclusion precipitation being a hindrance for dislocation movement.

Work was conducted with financial support of an RNF grant (project No. 19-79-10059).

REFERENCES

1. W. Yan, W. Chen, S. Zhang, et al., "Evolution of solidification structures and mechanical properties of high-Si Al alloys under permanent magnetic stirring," *Mater. Charact.*, **157**, 109894 (2019).
2. A. M. A. Mohamed A. M. Samuel, et al., "Influence of additives on the microstructure and tensile properties of near-eutectic Al – 10.8% Si cast alloy," *Mater. Design*, **30**, 3943 – 3957 (2009).
3. M. Javidani and D. Larouche, "Application of cast Al – Si alloys in internal combustion engine components," *Int. Mater. Rev.*, **59**(3), 132 – 158 (2014).
4. V. S., Zolotorevskiy, N. A. Belov, and M. V. Glazoff, *Casting Aluminum Alloys*, Elsevier Science, (2007).
5. M. Okayasu, K. Ota, and S. Takeuchi, "Influence of microstructural characteristics on mechanical properties of ADC12 aluminum alloy," *Mater. Sci. Eng. A*, **592**. 189 – 200 (2014).
6. C.-Y. Jeong, "High temperature mechanical properties of AlSiMg(Cu) alloys for automotive cylinder heads," *Mater. Trans.*, **54**, 588 – 594 (2013).
7. S. Hegde and K. N. Prabhu, "Modification of eutectic silicon in Al – Si alloys," *J. Mater. Sci.*, **43**, 3009 – 3027 (2008).
8. H. Xia, C. Zhang, P. Lv, et al., "Surface alloying of aluminum with molybdenum by high-current pulsed electron beam," *Nucl. Instruments Methods Phys. Res. Sect. B, Beam Interact. with Mater. Atoms*, **416**, 9 – 15 (2018).
9. S. V. Konovalov, K. V. Alsaraeva, V. E. Gromov, et al., "The influence of electron beam treatment on Al – Si alloy structure destroyed at high-cycle fatigue," *Key Eng. Mater.*, **675 – 676**, 655 – 659 (2016).
10. V. E. Gromov, Yu. F. Ivanov, S. V. Vorobiev, and S. V. Konovalov, *Fatigue of Steels Modified by High Intensity Electron Beams*, Cambridge International Science Publishing (2015).
11. G. Bo, X. Ning, and X. Pengfei, "Shock wave induced nanocrystallization during the high current pulsed electron beam process and its effect on mechanical properties," *Mater. Lett.*, **237**, 180 – 184 (2019).
12. L. Diankun, G. Bo, Z. Guanglin, et al., "High-current pulsed electron treatment of hypoeutectic Al – 10Si alloy" *High Temp. Mater. Proc.*, **36**(1), 97 100 (2017).
13. B. Gao, Y. Hao, W. F. Zhuang, et al., "Study on continuous solid solution of Al and Si elements of a high current pulsed electron beam treated hypereutectic Al17.5Si alloy," *Phys. Procedia*, **18**, 187 – 192 (2011).
14. Y. Hao, B. Gao, G. F. Tu, et al., "Improved wear resistance of Al – 15Si alloy with a high current pulsed electron beam treatment," *Nucl. Instruments Methods Phys. Res. Sect. B, Beam Interact. with Mater. Atoms*, **269**(13), 1499 – 1505 (2011).
15. H. Li, L. Zhan, M. Huang, et al., "Investigation on the asymmetric creep ageing behaviour of 2195-T84 Al – Li alloy under different tensile and compressive stress levels," *Intermetallics*, **131**, 107078 (2021).
16. X. X. Zhang, A. Lutz, H. Andrä, et al., "Evolution of microscopic strains, stresses, and dislocation density during in-situ tensile loading of additively manufactured AlSi10Mg alloy," *Int. J. Plasticity*, **139**, 102946 (2021).
17. G. Ozur and D. I. Proskurovsky, "A wide-aperture, low-energy, and high-current electron beam source with a plasma anode based on a reflective discharge," *Instr. Experim. Tech.*, **48**(6), 753 – 760 (2005).
18. D. Zaguliaev, S. Konovalov, Y. Ivanov, et al., "Microstructure and microhardness of piston alloy AK10M2N irradiated by pulsed electron beam," *Arch. Foundry Eng.*, **20**(3), 92 – 98 (2020).
19. S. Konovalov, D. Zaguliaev, Y. Ivanov, et al., "Modification of AK10M2H alloy surface by intensive pulsed electron beam," *J. Mater. Res. Technol.*, **9**(3), 5591 – 5598 (2020).
20. N. A. Belov, S. V. Savcheenko, and A. B. Khvan, *Silumin Phase Composition and Structure: Reference Edition* [in Russian], MISiS, Moscow (2007).
21. G. Thomas and M. J. Goringe, *Transmission Electron Microscopy of Materials*, Wiley, New York (1979).